Biochemical Pharmacology 81 (2011) 111–122

Contents lists available at ScienceDirect

Biochemical Pharmacology

journal homepage: www.elsevier.com/locate/biochempharm

A novel approach for stress-induced gastritis based on paradoxical anti-oxidative and anti-inflammatory action of exogenous 8-hydroxydeoxyguanosine

Chan Young Ock [a], Kyung Sook Hong [a], Ki-Seok Choi [a], Myung-Hee Chung [b], Yun soo Kim [c], Ju Hyun Kim [c], Ki-Baik Hahm [a,c,*]

[a] Lab of Translational Medicine, Gachon University of Medicine and Science Lee Gil Ya Cancer and Diabetes Institute, Songdo-dong 7-45, Yeonsu-gu, Incheon, Republic of Korea
[b] Department of Pharmacology, Seoul National University College of Medicine, Yongon-dong 28, Chungno-gu, Seoul, Republic of Korea
[c] Department of Gastroenterology, Gachon Graduate School of Medicine, Guwol-dong 1198, Namdong-gu, Republic of Korea

ARTICLE INFO

Article history:
Received 2 August 2010
Accepted 24 August 2010

Keywords:
8-Hydroxydeoxyguanosine
Water immersion restraint stress
NADPH oxidase
Rac-GTP
Oxidative stress

ABSTRACT

Reactive oxygen species (ROS) attack guanine bases in DNA and form 8-hydroxydeoxyguanosine (8-OHdG), which has been regarded simply as an oxidative mutagenic by-product. On the other hand, our previous report showed paradoxically ROS attenuating action of generated 8-OHdG. In the current study, both *in vitro* and *in vivo* experiments were executed in order to document anti-oxidative and anti-inflammatory actions of 8-OHdG in cell model and to elucidate the therapeutic efficacy against water immersion restraint stress (WIRS)-induced gastritis animal model. Electron spin resonance measurements showed that 8-OHdG at >5 μg/ml completely scavenged OH^- radicals, which was further confirmed by checking 2′-7′-dichlorodihydrofluorescein diacetate (DCFDA) spectroscopy. On molecular assay, 8-OHdG antagonized the action of GTP on Rac, a small GTP binding protein, without affecting Rac-guanosine exchange factor (GEF) or phosphoinositide 3-kinases (PI3K) activity. In Raw264.7 cells, 8-OHdG was found to be associated with marked attenuations of NOX1, NOXO1, and NOXA1 accompanied with the decreased expressions of LPS-induced inflammatory mediators including COX-2, iNOS, IL-1β, and IL-6. Similarly, 8-OHdG attenuated hypoxia-induced angiogenesis and platelet endothelial cell adhesion molecule-1 (PECAM-1), COX-2, iNOS, IL-8, and VEGF expressions in HUVEC cells. At transcriptional level, 8-OHdG inhibited the nuclear translocation of NF-κB, inhibitory κB kinase (IKK) β kinase activation, and decreased phospho-IκBα levels. 8-OHdG efficiently ameliorated WIRS-induced gastric mucosal injury as evidenced with improvement of gross lesion index and attenuation of engaging mediators. Taken together, exogenous 8-OHdG can be a functional molecule regulating oxidative stress-induced gastritis through either antagonizing Rac-GTP binding or blocking the signals responsible for gastric inflammatory cascade.

1. Introduction

When DNA is attacked by ROS, guanine is transformed into 8-oxo-7, 8-dihydroguanine (8-oxo-Gua), which is the most abundant oxidative DNA adduct [1,2] and 8-oxo-Gua in DNA can be detrimental due to its ability to induce transversion mutation [3,4]. Fortunately, mammalian cells have multiple repair systems that counteract the hazardous effects of 8-oxo-Gua. That is, 8-oxo-Gua in DNA is removed by, for example, base excision repair (BER) enzymes, like 8-oxo-guanine glycosylase (OGG1), or eliminated by a nucleotide excision repair (NER) mechanism. Consequently, 8-oxo-7, 8-dihydro-2′-deoxyguanosine (8-OHdG), a nucleoside of 8-oxo-Gua, is generated from either damaged oligomer which contains 8-oxo-Gua by NER or from cytoplasmic oxidized nucleotides, like 8-hydroxy-dGTP [5–7]. Since 8-OHdG, unlike any other species that contains oxidized guanine, is membrane

Abbreviations: ROS, reactive oxygen species; 8-OHdG, 8-hydroxydeoxyguanosine; WIRS, water immersion restraint stress; NOX, NADPH oxidase; Rac-GTP, a subfamily of the Rho family of GTPases; Rac-GEF, Rac-Guanosine exchange factor; NF-κB, nuclear factor-kappaB; HUVEC, human umbilical vein endothelial cell; DCFDA, 2′-7′-dichlorodihydrofluorescein diacetate; COX, cyclooxygenase; VEGF, vascular endothelial growth factor; PI3K, phosphoinositide 3-kinases; OGG1, 8-oxo-guanine glycosylase; TNF-α, tumor necrosis factor-alpha; OH, hydroxyl radical; IKK, IκB kinase; PECAM, platelet endothelial cell adhesion molecule; LPS, lipopolysaccharide; EMSA, electrophoretic mobility shift assay.

* Corresponding author at: Lab of Translational Medicine, Gachon University of Medicine and Science Lee Gil Ya Cancer and Diabetes Institute, 7-45 Songdo-dong, Yeonsu-gu, Incheon, 406-840, Republic of Korea. Tel.: +82 32 899 6055; fax: +82 32 899 6054.
E-mail address: hahmkb@gachon.ac.kr (K.-B. Hahm).

0006-2952/$ – see front matter © 2010 Elsevier Inc. All rights reserved.
doi:10.1016/j.bcp.2010.08.023

permeable [7], it is usually detected in the urine or sera of patients, which is generally acknowledged that 8-OHdG is regarded as biomarker for oxidative damage in diverse disease conditions including atherosclerosis [8], diabetes mellitus [9], various cancers [10,11] or *Helicobacter pylori*-associated gastritis [12]. Though exogenous treatment with 8-hydroxy-GTPγS (the permeable form of 8-hydroxy-GTP) has been reported to block the Rac1/Cdc42 pathway [13], the exact biologic significance of exogenous 8-OHdG administration has been described only in few publications. Our group were the first to suggest that exogenous treatment with 8-OHdG could paradoxically have anti-inflammatory effects on a brain microglia cell line by blocking the Rac1/STATs signaling pathway [14]. Subsequently, it was reported that 8-OHdG has a preventive effect on lipopolysaccharide (LPS)-induced inflammation in Balb/c mice [15], which raised the possibility that 8-OHdG could be used to treat oxidative stress-associated disease, as well as being a marker of oxidative stress.

Phagocytic leukocytes generate ROS, a process important for killing invading microorganisms, and the source of these oxidant generations is NADPH oxidase (NOX), a tightly controlled multicomponent enzyme composed of a membrane-associated catalytic moiety and cytosolic regulatory components, which should be assembled to form the active oxidase from several subunits. Phagocytic NOX is the first component of NOX system shown to be directly regulated by Rac-GTPase, which is known to be a critical ''molecular switch'' that regulates the formation of ROS by phagocytic leukocytes under either physiologic or pathologic conditions. In addition to NOX stimulation [16], Rac1 is known to play diverse roles, such as, inflammatory cascade transduction [17,18], cytoskeleton rearrangement, cell migration [19], cell growth, and apoptosis [20,21]. Rac1 activation is crucial for aggregating NOX complex, ROS production, and for turning on the Rac1 pathway, GDP bound at Rac1 in inactive states should be dislodged and GTP should be reloaded by Rac-Guanosine exchange factor (GEF) [31,32]. Though the upstream activator of Rac-GEF has not clearly been defined, it is believed by many that phosphoinositide 3-kinases (PI3K) might play a main role in enhancing GEF activity, and active GEF converts GDP into GTP [33,40,41].

Disease models associated with oxidative bursts and inflammatory bouts in the pathogenesis of stress-induced gastritis, a common problem in the intensive care unit setting or in out patient department of gastroenterology [22], can be proposed because the participating pathophysiologic mechanisms of stress-induced gastritis are local ischemia followed by reperfusion injury, inflammatory cell infiltrations, and muco-destructive changes [23–25]. Adaptive response to these hypoxic injuries after stress up-regulates angiogenic factors, such as, IL-8 and VEGF, in addition to the activation of redox-sensitive NF-κB [26,27]. Reperfusion injury produces abundant ROS, which further causes harmful injuries by turning on inflammatory pathways. Therefore, a strategy to minimize oxidative injury seems to be fundamentally required to prevent stress-induced gastritis.

Based on these backgrounds, in order to document the molecular mechanisms responsible for the anti-inflammatory and anti-oxidant effect of exogenous 8-OHdG, we examined the cascade of changes including inflammatory mediators in LPS-challenged Raw264.7 cells and hypoxia-induced HUVEC cells in the absence or presence of exogenous 8-OHdG. To estimate anti-oxidant activity, Rac1-GTP binding assays and 2′-7′-dichlorodihydrofluorescein diacetate (DCFDA) staining were performed and to evaluate anti-inflammatory effects, levels of NOXs, COX-2, and iNOS and activities of NF-κB pathway were determined. Finally, the *in vivo* pretreatment efficacy of exogenous 8-OHdG on rat model of water immersion restraint stress (WIRS)-induced gastritis was documented.

2. Materials and methods

2.1. Materials and cell cultures

LPS (*Escherichia coli* serotype O111: B4) and 8-OHdG were purchased from Sigma Aldrich (Saint Louis, MO). Anti-phospho-p85/p55 antibody, anti-p85 antibody, anti-phospho-*akt* antibody, anti-*akt* antibody, anti-phospho-IκBα antibody, anti-IκBα antibody were all purchased from Cell Signaling Technology (Danvers, MA) and anti-β-actin antibody, anti-lamin B antibody, anti-α-tubulin antibody, anti-p65 antibody were purchased from Santa Cruz Biotechnology (Santa Cruz, CA). COX-2 antibody was purchased from Thermo Fisher Scientific (Fremont, CA) and iNOS antibody was purchased from BD Bioscience, CA). Raw264.7 cells were purchased from ATCC (Manassas, VA), and HUVEC cells from InnoPharmaScreen (Asan, Korea). Raw264.7 cells, macrophage cell line, were cultured in Dulbecco's modified Eagle's medium (DMEM) containing 10% (v/v) fetal bovine serum, 100 U/ml penicillin, 100 μg/ml streptomycin and 25 mM HEPES and HUVEC cells, human endothelial cells, were cultured in M199 medium (InnoPharmaScreen). Cells were maintained at 37 °C in a humidified atmosphere containing 5% CO_2. 5.0×10^5/ml Raw264.7 cells or 1.0×10^5/ml HUVEC cells were seeded and incubated for 24 h, then media were changed for media containing 8-OHdG (0–500 μg/ml), and incubated for 2 h. Raw264.7 cells were then treated with LPS at 1 μg/ml and incubated for 0–24 h. HUVEC cells were moved to a 1% O_2 and 5% CO_2 hypoxic chamber and incubated for 0–12 h.

2.2. Electron spin resonance (ESR) spectroscopy

Various concentrations of 8-OHdG (0–200 μg/ml) added to a total volume of 200 μl containing 0.05 mM $FeSO_4$, 1 mM H_2O_2, 1 mM 5,5-dimethylpyrroline-N-oxide (DMPO, Sigma Aldrich, Saint Louis, MO), and 50 mM sodium phosphate at pH 7.4 at room temperature. Reactions were initiated by adding H_2O_2. After incubation for 1 min, aliquots of the reactions were transferred to a quartz cell and the spectrum of DMPO-OH was examined using an ESR spectrophotometer (JES-TE300, JEOL, Tokyo, Japan). Examinations were carried out under the following conditions: magnetic field, 338.0 ± 5.0 mT; microwave power, 4.95 mW; frequency, 9.421700 GHz; modulation amplitude, 5 mT; sweep time, 0.5 min; and time constant, 0.03 s.

2.3. ROS generation measurement

Treated cells were incubated with 10 μM DCFDA (Sigma Aldrich) for 30 min in chamber plates. After washing with PBS 3 times, cells were mounted using Prolong Gold antifade reagent (Invitrogen Life Technologies, Carlsbad, CA). Fluorescence was measured using a confocal laser microscope.

2.4. Rac1 activation assay and Rac-GEF activation assay

Rac activity was analyzed by determining the amount of GTP-bound Rac1 pulled-down by interacting GST-PAK-PBD (p21 activated kinase-protein binding domain) with Rac1 using the Rac1 activation assay (Cytoskeleton, Denver, CO), according to the manufacturer's instructions. Briefly, 400 μg protein extracts were diluted to 1 μg/μl, incubated with 20 μl of GST-PAK-PBD beads for 12 h at 4 °C, and washed with lysis buffer twice. Beads were then suspended in 5 μl of 5× loading dye, proteins were separated by SDS-PAGE, and transferred to PVDF membranes. GTP-bound Rac1 levels were determined using monoclonal mouse anti-Rac1 antibody. Guanine nucleotide exchange factor (GEF) activities were analyzed by determining the amount of Rac1 G15A (a constitutive-active-mutant of Rac1)-bound GEF pulled-down

using the Active Rac-GEF assay kit (Cell Biolabs, San Diego, CA). Briefly, protein extracts (400 μg) were diluted to 1 μg/μl and incubated with 20 μl of Rac1 G15A agarose beads for 12 h at 4 °C. Beads were washed with lysis buffer twice, suspended in 5 μl of 5× loading dye, and proteins were separated by SDS-PAGE and transferred to PVDF membranes. Active Rac-GEF levels were measured using polyclonal rabbit anti-Tiam1 antibody.

2.5. Western blot analysis

Treated cells were washed twice with PBS and then lysed in ice-cold cell lysis buffer (Cell Signaling Technology) containing 1 mM phenylmethylsulfonyl fluoride (PMSF, Sigma Aldrich). After 20 min of incubation, samples were centrifuged at 10,000 × *g* for 10 min. Supernatants were then collected. Proteins in lysates were separated by SDS-PAGE and transferred to polyvinylidene fluoride (PVDF) membranes, which were incubated with primary antibodies, washed, incubated with peroxidase-conjugated secondary antibodies, rewashed, and then visualized using an enhanced chemiluminescence (ECL) system (GE Healthcare, Buckinghamshire, UK).

2.6. Nuclear protein extraction and electrophoretic mobility gel shift assay (EMSA)

Nuclear and cytoplasmic fractions were extracted using NE-PER Nuclear and cytoplasmic reagents (Pierce, Rockford, IL), according to the manufacturer's instructions. The NF-κB oligonucleotide probe, 5′-AGT TGA GGG GAC TTT CCC AGG C-3′, (Promega, Madison, WI) was labeled with [γ-^{32}P] ATP using T4 polynucleotide kinase (Promega, Madison, WI) and separated from unincorporated [γ-^{32}P] ATP by gel filtration using a nick spin column (GE Healthcare). Before adding the ^{32}P-oligonucleotide (100,000 cpm), 10 μg of nuclear extract was kept on ice for 15 min in gel shift binding buffer [10 mM Tris–HCl (pH 7.5), 100 mM NaCl, 1 mM DTT, 1 mM EDTA, 4% (v/v) glycerol and 0.1 mg/ml of sonicated salmon sperm DNA]. To determine the sequence specificity of the NF-κB DNA interaction, we added an excess of unlabeled oligonucleotides. After 20 min of incubation at room temperature, 2 μl of 0.1% bromophenol blue was added, and samples were electrophoresed through 6% non-denaturing PAGE at 150 V in a cold room. Finally, gels were dried and exposed to X-ray film (Kodak, Rochester, NY).

2.7. Immunocytochemistry

Treated cells in chamber slides were fixed by 3.7% formaldehyde for 15 min. After washing, cells were blocked in 5% BSA solution containing 0.1% Triton X-100 in PBS for 1 h at room temperature, and then incubated with primary antibody (1:100) for 12 h at 4 °C. Cells were then washed 3 times, incubated with secondary antibody (1:300) for 1 h, and then with 4'-6-diamidino-2-phenylindole (DAPI, 100 ng/ml) for 1 min at room temperature. After washing 5 times, cells were mounted with Prolong Gold antifade reagent (Invitrogen Life Technologies, Carlsbad, CA). Fluorescence was visualized under a confocal laser microscope (LSM710, Carl Zeiss, Oberkochen, Germany).

2.8. IKKβ kinase assay

Total cell lysates were extracted as described above. Cell lysates (200 μl) and anti-IKKβ antibody (1:50, Cell Signaling #2678, Cell Signaling Technology) were incubated with gentle rocking overnight at 4 °C. Then 20 μl of protein A/G agarose beads (sc-2003, Santa Cruz Biotechnology) were added, and the mixture was incubated with gentle rocking for 6 h at 4 °C. After washing twice with cell lysis buffer and with kinase buffer (Cell Signaling Technology #9802), pellets were suspended in 50 μl kinase buffer containing 1.5 μM biotin-tagged IκBα (Cell Signaling Technology #1146) and 20 μM ATP (Cell Signaling Technology #9804) and incubated for 30 min at room temperature. The kinase reaction was stopped by adding 50 μl of 50 mM EDTA, and mixtures were transferred into 96-well streptavidin-coated microplates (Nunc, Rochester, NY) and incubated at room temperature for 60 min. After washing 3 times, wells were incubated with anti-phospho-IκBα (1:1000, Cell Signaling Technology #2859) in 1% BSA PBS/T for 2 h at room temperature. After washed 3 times, each well was incubated with HRP-labeled anti-rabbit antibody (1:1000, Santa Cruz, sc-2004) for 30 min at room temperature. After washing another 3 times, TMB (Cell Signaling Technology #7004) solution was added, incubated for 10 min, and then the reaction was stopped by adding Stop solution (Cell Signaling Technology #7002). Fluorescence was read at 450 nm using a microplate reader.

2.9. RNA isolation and RT-PCR

After incubation, media was removed by suction and cells were washed with Dulbecco's phosphate-buffered saline (DPBS) twice. RiboEX (500 μl; GeneAll, Seoul, Korea) was added to plates, which were then incubated for 10 min at 4 °C. RiboEX was harvested and placed in a 1.5 ml tube, and 100 μl of chloroform was added and gently mixed. After incubation for 10 min in ice, samples were centrifuged at 10,000 × *g* for 30 min. Supernatants were extracted and mixed with 200 μl of isopropanol, and mixtures were incubated at 4 °C for 1 h. After centrifuging at 13,000 × *g* for 30 min, pellets were washed with 70% (v/v) ethanol. After allowing the ethanol to evaporate completely, pellets were dissolved in 100 μl of diethylene pyrocarbonate (DEPC)-treated water (Invitrogen Life Technologies). cDNA was prepared using reverse transcriptase originating from Murine-Moloney leukemia virus (Promega), according to the manufacturer's instructions. PCR was performed over 30 cycles of: 94 °C for 20 s, 58 °C for 30 s, and 72 °C for 45 s. Oligonucleotide primers were purchased from Bioneer (Seoul, Korea). The sequences of PCR primers used were as follows: forward, 5′-AAT GTA TCC GTT GTG GAT CT-3′ and reverse, 5′-TCC ACC ACC CTG TTG CTG TA-3′ for mouse GAPDH; forward, 5′-CAT CCT GCC AGC TCC ACC GC-3′ and reverse, 5′-GGG AGG AAG GGC CCT GGT GT-3′ for mouse COX2; forward, 5′-GTG GTG ACA AGC ACA TTT GG-3′ and reverse, 5′-GGC TGG ACT TTT CAC TCT GC-3′ for mouse iNOS; forward, 5′-GGG ATG ACC ATA AGG GGA GT-3′ and reverse, 5′-CCC AAC CAG TAC AGC CAC TT-3′ for mouse NOX1; forward, 5′-TCC CTG TGT ACA GCC TTT CC-3′ and reverse, 5′-AGT GCA GAA CTG CCT CCC TA-3′ for mouse NOXO1; forward, 5′-TTA CTG TGC CCC TGA AGG TC-3′ and reverse, 5′-CAC AGA ACA TCC ACC GTG TC-3′ for mouse NOXA1; forward, 5′-ATA GGC GTT TTC CTG TGT GG-3′ and reverse, 5′-CTG GCA TGT CAA AGG GAA AT-3′ for mouse NOX2; forward, 5′-ATA ACG GGC GTA GGG AGT CT-3′ and reverse, 5′-CCG GAG TTA CAG GCA AAT GT-3′ for mouse p47^{phox}; forward, 5′-CTT CAA CAT AGG CTG CGT GA-3′ and reverse, 5′-CTT CAT GTT GGT TGC CAA TG-3′ for mouse p67^{phox}; forward, 5′-CAG GCT CCG AGA TGA ACA ACA AAA-3′ and reverse, 5′-TGG GGA ACT CTG CAG ACT CAA ACT-3′ for mouse IL-1β; forward, 5′-CCG GAG AGG AGA CTT CAC AG-3′ and reverse, 5′-TGG TCT TGG TCC TTA GCC AC-3′ for mouse IL-6; forward, 5′-AGG TCG GAG TCA ACG GAT TTG G-3′ and reverse, 5′-ACA GTC TTC TGG GTG GCA GTG ATG-3′ for human GAPDH; forward, 5′-GGT CTG GTG CCT GGT CTG ATG ATG-3′ and reverse, 5′-GTC CTT TCA AGG AGA ATG GTG C-3′ for human COX2; forward, 5′-GGC CTC TCA GCT CAC CCC GA-3′ and reverse, 5′-CCA GGC GCA CTG TCT GGT GG-3′ for human iNOS; forward, 5′-TGG GTG CAG AGG GTT GTG-3′ and reverse, 5′-CAG ACT AGG GTT GCC AGA TTT A-3′ for human IL-8; and forward, 5′-TCG GGC CTC CGA AAC CAT G-3′ and reverse, 5′-GGT TCC CGA AAC CCT GAG G-3′ for human VEGF.

2.10. In vitro angiogenesis assay

This assay was performed using a commercial kit according to the manufacturer's instruction (Millipore, Billerica, MA). Briefly, ECMatrix and Diluent buffer were mixed to make a solid gel, which was then plated in 96-well microplates. Human umbilical vein endothelial cells (HUVEC, 1.0×10^5/ml) were seeded with 8-OHdG (0–250 μg) then incubated at 37 °C for 4 h. Sprouting tube formation was observed under a light microscope.

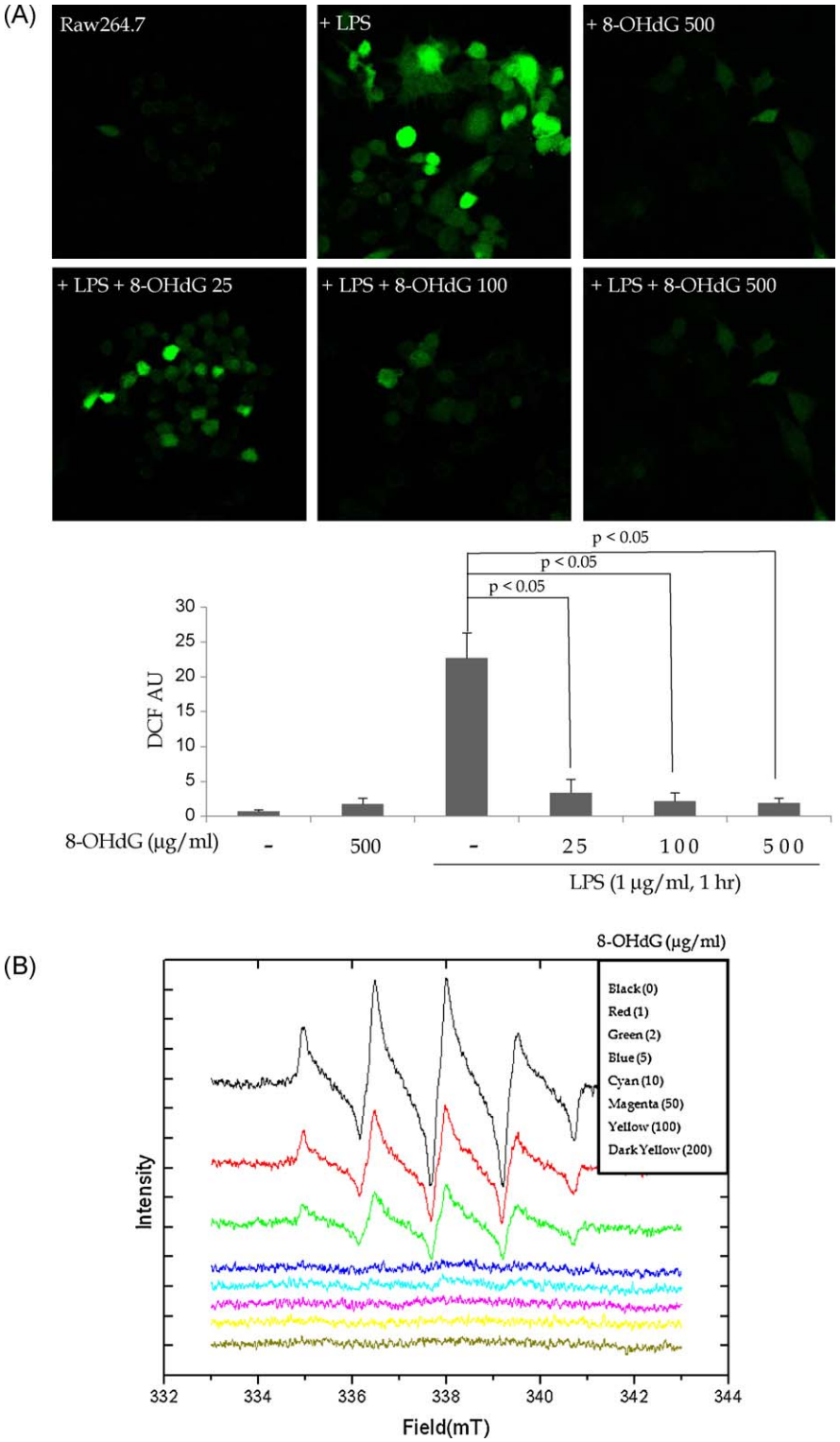

Fig. 1. The anti-oxidative effect of 8-OHdG. (A) Raw264.7 macrophages were treated with 0–500 μg/ml 8-OHdG for 2 h before LPS stimulation (1 μg/ml, 30 min), and then incubated with $DCFH_2$-DA 10 μM for 30 min. Intracellular ROS accumulation was measured using a confocal laser microscope. Fluorescence intensities were measured using a densitometer. (B) 8-OHdG (1–200 μg/ml) was in a total volume of 200 μl containing 0.05 mM $FeSO_4$, 1 mM H_2O_2, 1 mM 5,5-dimethylpyrroline-N-oxide (DMPO) and 50 mM sodium phosphate at pH 7.4 and 37 °C. Reactions were initiated by adding H_2O_2, and after 1 min of incubation, aliquots of reaction mixtures were transferred to crystal cuvetes. ESR was used to quantify DMPO-OH levels. Hydroxyl radical levels were observed to decrease dose dependently with 8-OHdG concentration higher than 5 μg/ml.

2.11. Induction of water immersion restraint stress (WIRS) and treatments with 8-OHdG

Six-week-old specific-pathogen-free Sprague-Dawley male rats (Charles River Laboratories, Tokyo, Japan) were used for the experiments. A total of 24 rats were fed a sterilized commercial pellet diet (Biogenomics Co., Seoul, Korea), given sterile water *ad libitum*, and housed in an air-conditioned room under a 12 h light/dark cycle. The 24 rats were divided into three groups, 8 rats per group, respectively; a non-treated control group, a water immersion restraint stress (WIRS) for 10 h treated group, and an 8-OHdG (50 mg/kg) administered 1 h before WIRS group. The rationale for oral administration of 50 mg/kg 8-OHdG dissolved in 0.5% carboxylmethyl cellulose (CMC) 1 h before WIRS came from our preliminary study showing that 50 mg/kg was efficacious in animal model of inflammatory bowel disease provoked with either dextran sulfate sodium in drinking water or intrarectal administration of TNBS 1 h before these damaging causes (Supplementary Fig. 1). Animals were handled in an accredited animal facility in accordance with Association for Assessment and Accreditation of Laboratory Animal Care International (AAALAC International) guidelines under the facility named CACU (The Center of Animal Care and Use) of Gachon University Lee Gil Ya Cancer and Diabetes Institute after IRB approval. Animals were deprived of food, but allowed free access to water 24 h before exposure to WIRS. To induce WIRS, rats were restrained in wire cages and immersed up to the depth of the xiphoid process in a water bath at 23 °C for 10 h. Animals were killed immediately after water immersion. The supporting backgrounds that stomachs were removed, opened along the greater curvature, and rinsed with phosphate-buffered saline. Isolated tissues were subjected to a histological examination, ELISA, and Western blotting. Bleeding indices were evaluated using formalin-fixed sections and bleeding rates (%) were calculated, as described by Yamamoto et al. [28] In this study, an index of 0 means no bleeding; an index of 1 means mild bleeding (the presence of small amounts of coagula in the stomach); an index of 2 means moderate bleeding (intermediate between index 1 and 3); and an index of 3 means severe bleeding (stomach were filled with blood including coagula). Pathological lesion indices were defined as previously described [29]; ischemic necrosis was rated as 0–3 (1 = none or mild, 2 = moderate, and 3 = severe), hemorrhage as 0–3 (0 = none, 1 = mild, 2 =moderate, 3 = severe), the number of mucoid cap composed of necrotic debris as 0–3 (0 = $<$ 1, 1 = 1–2, 2 = 3–4, 3 = $\geq$5), and the maximal size of mucosal defects as 0-3 (0 = 0, 1 = $<$ 500 μm, 2 = 500–1000 μm, and 3 = $>$1000 μm).

2.12. Measurement of TNF-α, IL-1β, VEGF, PGE_2, total nitrate, and gastrin I levels in gastric tissues

Stomach tissues were homogenized with 1 ml of cell lysis buffer (Cell Signaling Technology) containing 1 mM of PMSF, incubated for 20 min, and centrifuged at 10,000 × *g* × 10 min. Supernatants were re-centrifuged and collected. All samples were stored in −80 °C until required. Rat TNF-α and Rat IL-1β (BioSource, Life Technologies, Carlsbad, CA), Rat VEGF and PGE_2 (R&D Systems, Minneapolis, MN), Nitrate/Nitrite (Cayman Chemical Company, Ann Arbor, MI), and Rat Gastrin I (Assay Designs, Ann Arbor, MI) ELISAs were performed according to manufacturers' instructions.

2.13. Statistical analysis

The data are presented as means ± standard deviations (SD). The Tukey test or the Student's *t* for unpaired results was used to evaluate differences between more than three groups or between two groups, respectively. Differences were considered to be significant for values of $p < 0.05$.

3. Results

3.1. Paradoxical anti-oxidative actions of exogenous 8-OHdG

In order to determine whether exogenous 8-OHdG, of which levels were well-known as biomarker for oxidative stress or related mutagenesis [30], acts paradoxically as an anti-oxidant, 2′-7′-dichlorodihydrofluorescein diacetate (DCFDA) staining of LPS-challenged Raw264.7 cells was examined under a confocal microscope. LPS stimulation produced significant DCF fluorescence, suggesting excessive amounts of oxygen free radicals were generated in Raw264.7 cells (Supplementary Fig. 3). However, exogenous 8-OHdG significantly attenuated DCF-induced fluorescence, signifying that 8-OHdG had an anti-oxidative effect (Fig. 1A). Since ESR is generally acknowledged to provide the best means of observing hydroxyl and singlet oxygen generation directly, we used ESR measurement to examine the scavenging effects of different doses of 8-OHdG (0–200 μg/ml). DMPO was used as an adductor of hydroxyl radicals for this ESR study. As shown in Fig. 1B, 8-OHdG at $>$5 μg/ml exerted a marked radical scavenging effect. This experiment showed that 8-OHdG can act as an anti-oxidant in LPS-activated macrophages.

We, then, explored the molecular mechanisms responsible for the anti-oxidative effect of 8-OHdG in LPS activated macrophages. Since Rac1 activation is crucial for aggregating NOX complex and oxidized guanine like 8-OHdG might interfere Rac1-GTP binding [31,32], we hypothesized that 8-OHdG might down-regulate Rac1-GTP binding without affecting Rac-GEF activity to block the signal transduction required to generate inflammatory mediators. Before this, we checked whether 8-OHdG interfered with the initiation of PI3K signaling, because Rac1-GEF activity is known to be regulated by the PI3K pathway in the LPS-induced inflammatory cascade [33]. As shown in Fig. 2A and B, LPS challenge was found to be associated with the activation of PI3K-Akt, but 8-OHdG did not affect the activation of PI3K-Akt. The level of p-p85 (the main action domain of PI3K) though activated with LPS challenge, was not changed by 8-OHdG treatment. On the other hand, LY294002 (a potent PI3K inhibitor) reduced Rac-GEF activation, whereas 8-OHdG did not (Fig. 2C), suggesting that 8-OHdG might block LPS-associated Rac-GTPase activation rather than GEF or upstream PI3K. We also examined whether 8-OHdG could block LPS challenge associated Rac1 activation by immunoprecipitation (IP)-Western blot analysis (Fig. 2D). As shown in Fig. 2D, LPS challenge was associated with Rac1 activation, but 8-OHdG administration significantly inhibited Rac1 activation without influencing Rac-GEF activity, suggesting that LPS challenge might lead to the activations of NOXs via Rac1 activation, and that 8-OHdG might inhibit these activations.

3.2. Paradoxical anti-inflammatory actions of exogenous 8-OHdG

Before examining whether 8-OHdG can down-regulate the expressions of NOXs and inflammatory mediators, the levels of NOXs were measured at different time points after LPS challenge (Fig. 3A). LPS treatment increased the expression levels of NOXs: NOX1, NOXO1 (NADPH oxidase organizer 1), and NOXA1 (NADPH oxidase activator 1) at 6 h, whereas the expression levels of NOX2, $p47^{phox}$, and $p67^{phox}$ were unchanged in Raw264.7 cells after stimulation for 24 h. However, as shown in Fig. 3B, 8-OHdG dramatically inhibited the expressions of these NOXs: NOX1, NOXO1, and NOXA1 in a dose-dependent manner. In accordance with this NOX inhibition, 8-OHdG also reduced the expressions of LPS-induced COX-2, iNOS, IL-1β, and IL-6 mRNA (Fig. 3C). These inhibitions of COX-2 and of the iNOS transcript were further documented by Western blotting (Fig. 3D).

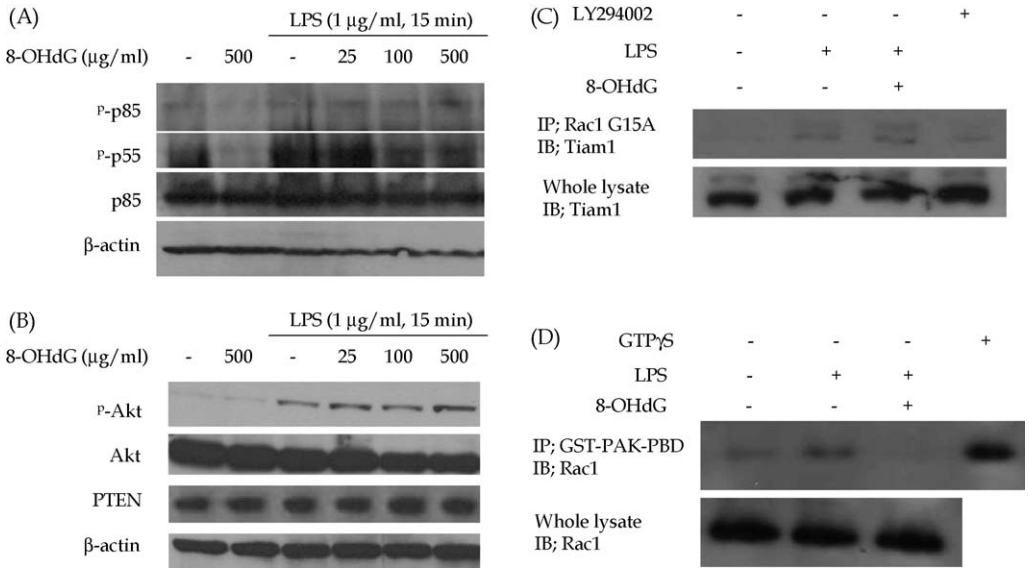

Fig. 2. 8-OHdG inhibited Rac1-GTP binding without affecting PI3K/Rac-GEF activity. (A) Raw264.7 cells were pretreated with 8-OHdG at 25, 100, and 500 μg/ml for 2 h and then LPS (1 μg/ml) was challenged for 15 min. Western blotting was performed using anti-phospho-p85/p55, anti-p85, and anti-β-actin. It was found that 8-OHdG did not affect PI3K levels. (B) Using the conditions detailed in A, changes in phosphorylated Akt, Akt, and PTEN level were measured using anti-phospho-Akt, anti-Akt, anti-PTEN, and anti-β-actin antibody, respectively. However, the results obtained showed that 8-OHdG did not influence the PI3K signal pathway. (C) Raw264.7 cells were pretreated with or without 8-OHdG 500 μg/ml or LY294002 50 μM for 2 h and then LPS (1 μg/ml) was challenged for 5 min. Rac-GEF activity was assayed by immunoprecipitation using Rac1 G15A agarose beads. (D) Rac1-GTP binding was assayed by immunoprecipitation using GST-PAK-PBD beads. GTPγS (200 μM) incubated with cell lysates for 15 min at 30 °C was used as a positive control.

3.3. Anti-angiogenic actions of exogenous 8-OHdG

To cope with hypoxia associated with inflammation, vascular endothelial cells readily form new vessels to deliver more oxygen. Because 8-OHdG can effectively inhibit the inflammatory cascade and oxidative stress, we hypothesized that 8-OHdG might attenuate hypoxia-induced angiogenesis in HUVECs. After 4 h of incubation in hypoxic chamber, HUVECs transformed into tubular forms and platelet endothelial cell adhesion molecule-1 (PECAM-1) expression was increased. However, 8-OHdG v treatment dramatically inhibited hypoxia-induced tubular formation and PECAM-1 expression (Fig. 4A and B). Moreover, the expressions of inflammatory mediators, such as, COX-2 and iNOS, as well as those of pro-angiogenic mediators, such as, IL-8 and VEGF, were blocked in 8-OHdG treated HUVECs (Fig. 4C).

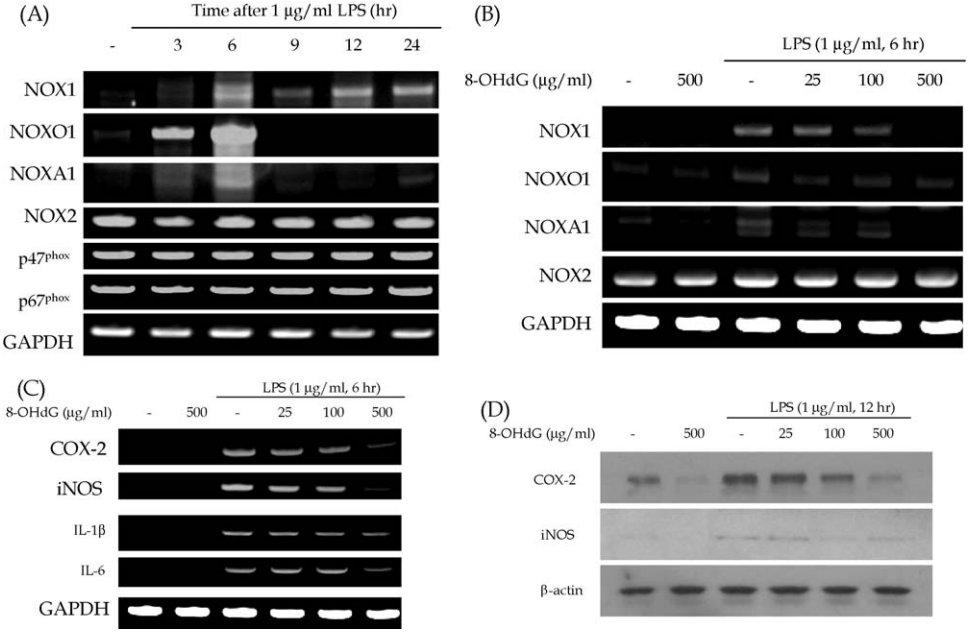

Fig. 3. 8-OHdG inhibited NOX subunits and inflammatory mediators in LPS-challenged Raw264.7 cells. (A) Raw264.7 cells were challenged with LPS (1 μg/ml) for different times. The expressions of the NOX subunits, NOX1, NOXO1, NOXA1, and NOX2, were assayed by RT-PCR. (B) The expressions of NOX subunits were assayed after pretreatment with 25, 100, and 500 μg/ml of 8-OHdG for 2 h and stimulation with LPS (1 μg/ml) for 6 h. 8-OHdG efficiently attenuated the expression of NOX1, but not that of NOX2. (C) The expressions of inflammatory mediators were assayed after pretreatment with 8-OHdG at 25, 100, and 500 μg/ml for 2 h and stimulation with LPS (1 μg/ml) for 6 h. 8-OHdG was found to efficiently attenuate the expressions of COX-2, iNOS, IL-1β, and IL-6. (D) After 12 h of LPS (1 μg/ml) treatment, COX2, iNOS expressions were assayed by Western blotting using anti-COX2 and anti-iNOS antibody.

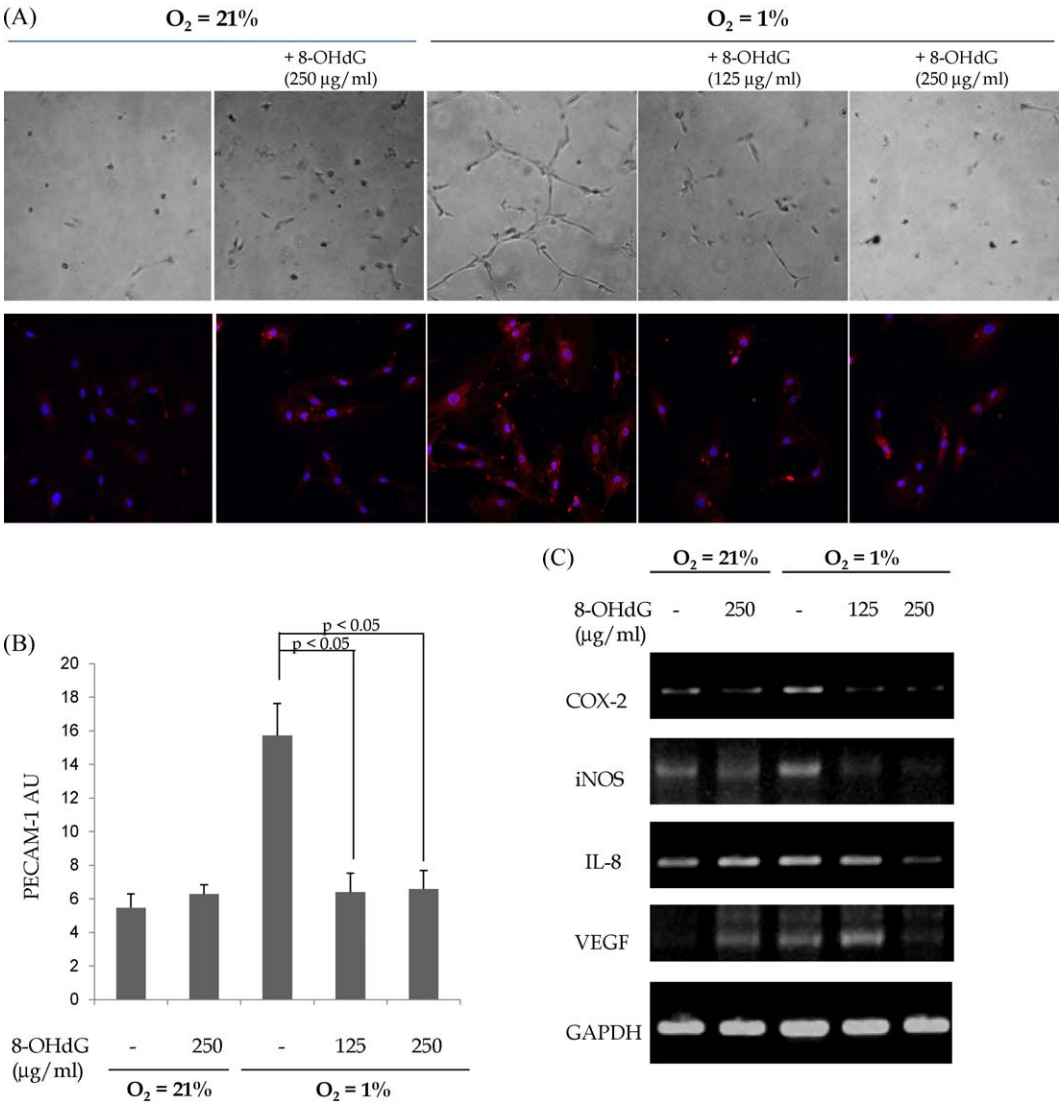

Fig. 4. 8-OHdG inhibited hypoxia-induced angiogenesis and the expressions of angiogenesis-related mediators in HUVEC cells. 8-OHdG (0–250 μg/ml) was pretreated for 2 h and then cells were moved to a hypoxic chamber (1% O_2). (A) After 4 h in the hypoxic chamber, HUVEC growth in extracellular matrix (ECM)-mimic material was observed under a light microscope. After 12 h in the hypoxic chamber, PECAM-1 expressions in HUVEC cells were assayed by immunocytochemistry under a confocal laser microscope. (B) Relative PECAM-1 fluorescences were measured by densitometry. (C) After 6 h in the hypoxic chamber, the expressions of COX-2, iNOS, IL-8, and VEGF was assayed by RT-PCR.

3.4. Transcriptional repression by exogenous 8-OHdG

In determine whether the anti-oxidative effect of 8-OHdG could also attenuate the redox-related inflammatory pathway, we examined whether 8-OHdG inhibits redox-related transcriptional activations using EMSA, IKKβ kinase assays, and confocal imaging of NF-κB subunits. EMSA showed that LPS challenge significantly activated NF-κB-DNA binding, whereas 8-OHdG attenuated these activations (Fig. 5A). These findings were reinforced by measuring IκBα phosphorylation. As shown in Fig. 5B, LPS challenge decreased total amounts of IκBα consequent to increased phosphorylation of IκBα, which led to an increase in NF-κB activation. However, 8-OHdG inactivated IκBα phosphorylation in a dose-dependent manner, and the nuclear translocation of NF-κB p65 was decreased in Raw264.7 cells treated with 8-OHdG (Fig. 5C). These results were also confirmed by confocal imaging study stained with a p65 (Fig. 5D). In addition, IKKβ kinase assays (Fig. 5E) showed that 8-OHdG at ≥500 μg/ml significantly inhibited IKKβ activity, and this prevented the activation of NF-κB.

3.5. The therapeutic efficacy of exogenous 8-OHdG; WIRS-induced gastric damages

In order to examine the clinical application of the anti-inflammatory and anti-oxidative actions of 8-OHdG, we administered 8-OHdG to stress-induced gastritis model (Fig. 6A), because the fundamental pathogenic bases of WIRS-induced gastric damages have been reported to be oxidative stress related ischemia/reperfusion, inflammatory infiltration, and deranged regeneration [34,35]. Restraint stress for 10 h caused marked gastric mucosal damages, including multiple hemorrhagic streaks, ulcerations, and bleeding (Fig. 6B). Under the microscopic, WIRS-induced overt ulceration, coagulation necrosis, erosions, mucosal hemorrhages, and submucosal edema. 8-OHdG treatment 1 h before WIRS significantly improved gross lesion indices and pathologic lesion indices, as shown in Fig. 6C ($p < 0.05$). Furthermore, WIRS-associated gastric damages were associated with significant increases in mucosal TNF-α, IL-1β, and VEGF in addition to an increase in serum total nitrate (Fig. 6D). Further-

more, the attenuated gastric mucosal damages observed in the 8-OHdG group were found to be significantly associated with decreases in mucosal TNF-α and VEGF, which confirmed the previous *in vitro* results of regarding the protective effect of 8-OHdG under oxidative, inflammatory conditions (Fig. 7). Compared to other drugs prescribed clinically, rebamipide or *Artemisia asiatica*, 8-OHdG showed significantly higher protection from WIRS-induced gastric mucosal damages assessed with gross lesion index, pathological lesion index, and inflammatory cytokines (Supplementary Fig. 2).

4. Discussion

In this study, we found that the anti-oxidative and anti-inflammatory activities of exogenous 8-OHdG against LPS-induced ROS production were due to reduced Rac-GTP binding, and that exogenous 8-OHdG did not affect Rac-GEF activity or PI3K. Furthermore, exogenous 8-OHdG reduced ROS productions, attenuated the NF-κB signal pathway even under LPS stimulation, and reduced the expressions of pro-inflammatory mediators such as IL-1β, IL-6, COX-2, and iNOS in addition to the expressions of NOX1, NOXO1, and NOXA1. Based on this *in vitro* data, we examined the effect of exogenous 8-OHdG on WIRS-induced gastritis rat model, and it was found that 8-OHdG remarkably prevented WIRS-induced gastritis more than other kinds of mucoprotectant (Supplementary Fig. 2). These beneficial effects of exogenous 8-OHdG indicate that synthetic 8-OHdG can be viewed as a potential therapeutic for the treatment of various oxidative stress-associated diseases.

ROS are generated from diverse sources, such as, mitochondria, cytochrome P-450, peroxisomes, and other cellular elements under normal physiologic conditions [36–38], but in pathological situations the main source of ROS is NADPH oxidase (NOX) complex. NOX is a subset of enzymes involved in the oxidation of NADPH to $NADP^+$, which produces ROS as a by-product. Members of this subset include $gp91^{phox}$, $p47^{phox}$, $p67^{phox}$, $p40^{phox}$, $p22^{phox}$, and Rac1, and are present in the cytoplasm under normal conditions, but are recruited to the plasma membrane when they are activated [39]. In the present study, we found that the active form of the Rac-GEF fraction is decreased by LY294002 (a potent PI3K inhibitor), but Rac-GEF activity remained unchanged in the 8-OHdG treatment group, which suggests that PI3K is a crucial activator of Rac-GEF [40,41]. However, the feasible target of 8-OHdG is downstream of Rac-GEF in LPS-induced Raw264.7 cells. Because the Rac-GTP fraction was dramatically lower in the 8-OHdG treatment group, the main mechanism of attenuating Rac1

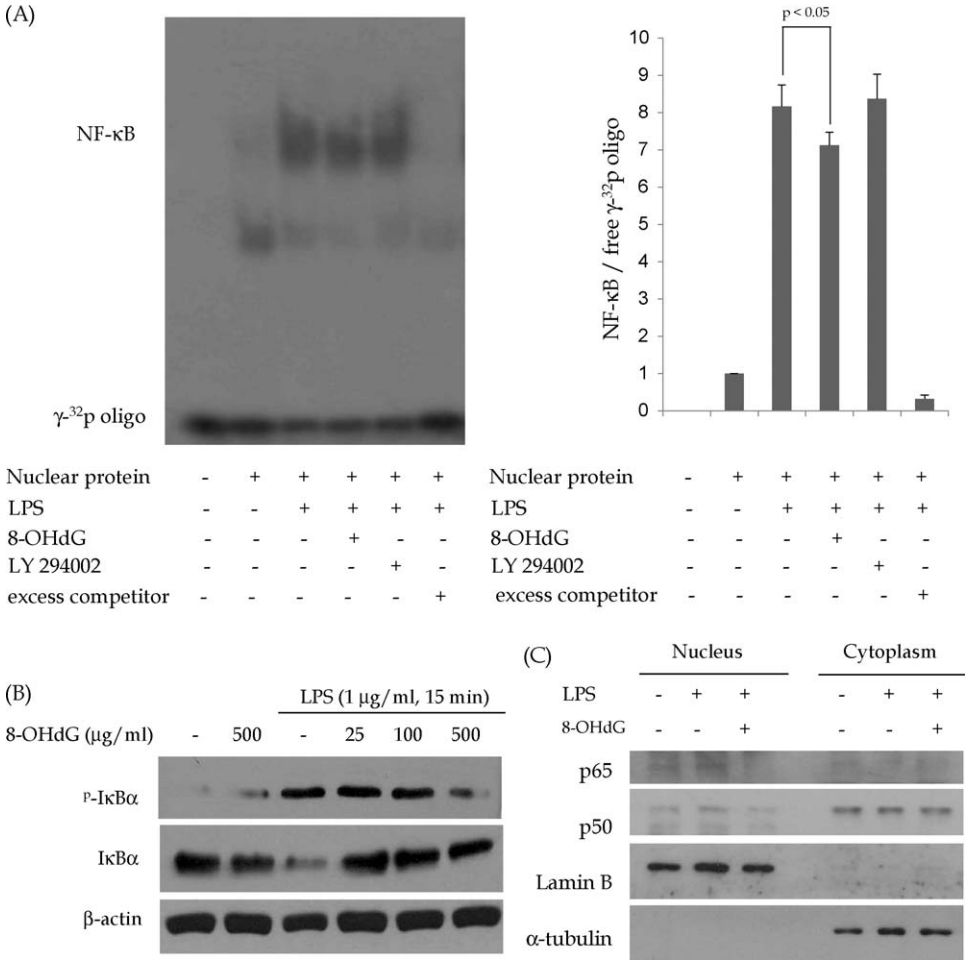

Fig. 5. 8-OHdG inhibited the NF-κB pathway in LPS stimulated Raw264.7 cells. (A) Raw264.7 cells were pretreated with or without 8-OHdG 500 μg/ml or LY294002 50 μM for 2 h and then LPS (1 μg/ml) was challenged for 30 min. Nuclear extracts were analyzed for NF-κB activity by EMSA in the presence or absence of an excess of cold probe (excess competitor). The relative intensities of NF-κB/free γ-^{32}p probe were determined by densitometry. (B) Raw264.7 cells were pretreated with 8-OHdG (0–500 μg/ml) for 2 h and then challenged with LPS (1 μg/ml) 15 min. Western blotting was performed using anti-phospho-IκBα, anti-IκBα, and anti-β-actin. (C) Raw264.7 cells were pretreated with or without 8-OHdG 500 μg/ml for 2 h and then challenged with LPS (1 μg/ml) for 30 min. Nuclear extracts were immunoblotted with anti-p65, anti-p50, Lamin B, and α-tubulin. (D) Raw264.7 cells were pretreated with or without 500 μg/ml 8-OHdG or 25 μM MG132 for 2 h and then challenged with LPS (1 μg/ml) for 30 min. The nuclear translocation of p65 was assayed by immunocytochemistry using a confocal laser microscope. (E) Raw264.7 cells were pretreated with 8-OHdG (0–500 μg/ml) for 2 h and then challenged with LPS (1 μg/ml) for 5 min. IKKβ kinase activity was assayed using biotin-tagged IκBα.

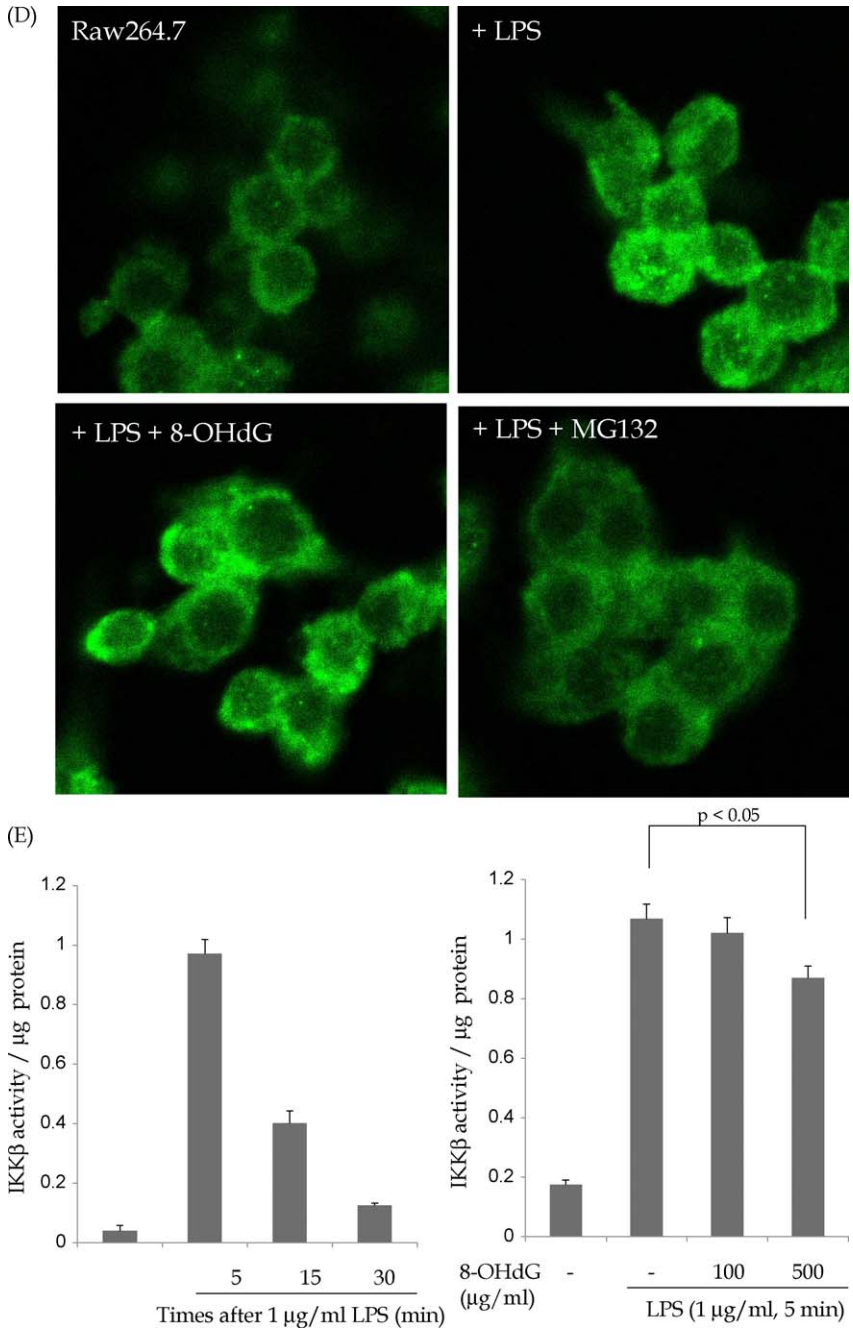

Fig. 5. (*Continued*).

activity by 8-OHdG might occur via the blocking of Rac-GTP binding in a competitive manner. Although structurally different from 8-OHdG, another oxidized form of guanine base, 8-hydroxy-GTPγS has been suggested to act as a competitive inhibitor of Rac-GTP [13].

NOX is a subset of enzymes responsible for ROS generation under pathological conditions and generates ROS to resolve bacterial infections by inducing "respiratory burst" in phagocytes [42,43]. Since NOX1 is expressed in colon [44], smooth muscle [45] and endothelial cells [46], the pathologic role of NOX1 has been implicated in various diseases, such as, vascular [47,48] and gastrointestinal (GI) diseases [49]. Among GI diseases, Kawahara et al. [50] showed increased expressions of NOX1 and NOXO1 in *H. pylori*-induced gastric mucosa cells, which suggests that *H. pylori*-induced gastritis is mediated by ROS generated by NOX [49]. However, the roles played by NOX and ROS in the pathologic progress of the types of gastric inflammation, like, NSAID-induced gastritis and stress-induced gastritis, have not been elucidated.

In 1957, Berendes et al. [51] recognized a rare syndrome in young boys who suffered from recurrent pyogenic infections with aberrant granulomatous reactions. This genetic disorder was later named chronic granulomatous disease (CGD). In these patients, it was reported that CGD phagocytes have diminished bactericidal capacity, such that respiratory burst is absent, although other functions of phagocytes, such as, chemotaxis, phagocytosis, and degranulation, remained intact [52]. Royer-Pokora et al. cloned the gene coding for the catalytic subunit of phagocytic NOX, originally referred to as $gp91^{phox}$, but now called NOX2 [42]. NOX1 is another subtype of NOX, which has been reported to be up-regulated in a *H. pylori*-induced gastritis model [50]. To activate NOX complex and produce ROS, NOX2 must be complexed with other NOX subunits, such as, $p47^{phox}$ and $p67^{phox}$. Similarly, NOX1 must interact with

NOXO1 and NOXA1, which share homology with $p47^{phox}$ and $p67^{phox}$, respectively. *In vitro* evidence has shown that co-transfection with NOX1, NOXO1, and NOXA1 results in production of abundant ROS even in the absence of stimulation [53]. In LPS-induced Raw264.7 cells, we observed that RNA expressions of NOX1, NOXO1, and NOXA1 were increased, while NOX2, $p47^{phox}$, and $p67^{phox}$ RNA expressions were unchanged. One interesting observation was that the ROS production as measured using the DCFDA assay versus time curve had two peaks, an early peak at less than 1 h after LPS stimulation, and other higher peak at 8–12 h (Supplementary Fig. 3). We explain this as follows: Raw264.7 cells are phagocytes, which constitutionally express NOX2. Thus, the early short-lived production of ROS is likely to be mediated by NOX2. The produced ROS would then activate various inflammatory pathways, such as, the NF-κB pathway. The second peak then could be due to up-regulations of NOX1, NOXO1, and NOXA1.

The term "stress" is widely used word, and in particular, stress is viewed as an important aspect of modern human life [54]. However, the definition of stress is somewhat ambiguous, and is perhaps best defined in a biologic sense, as the stimulus that drives an organism to adapt to new conditions [55]. The biologic mechanism of the "generalized alarm reaction", a host response to stressors, is explained as an alteration of the hypothalamus–pituitary–adrenal axis, a deranged immune response, and disturbed hormonal homeostasis, primarily of the glucocorticoid system [54]. Furthermore, it is recognized that severe stress can cause gastric damage [56], and although the incidence and the severity of stress-related mucosal diseases (SRMDs) have de-

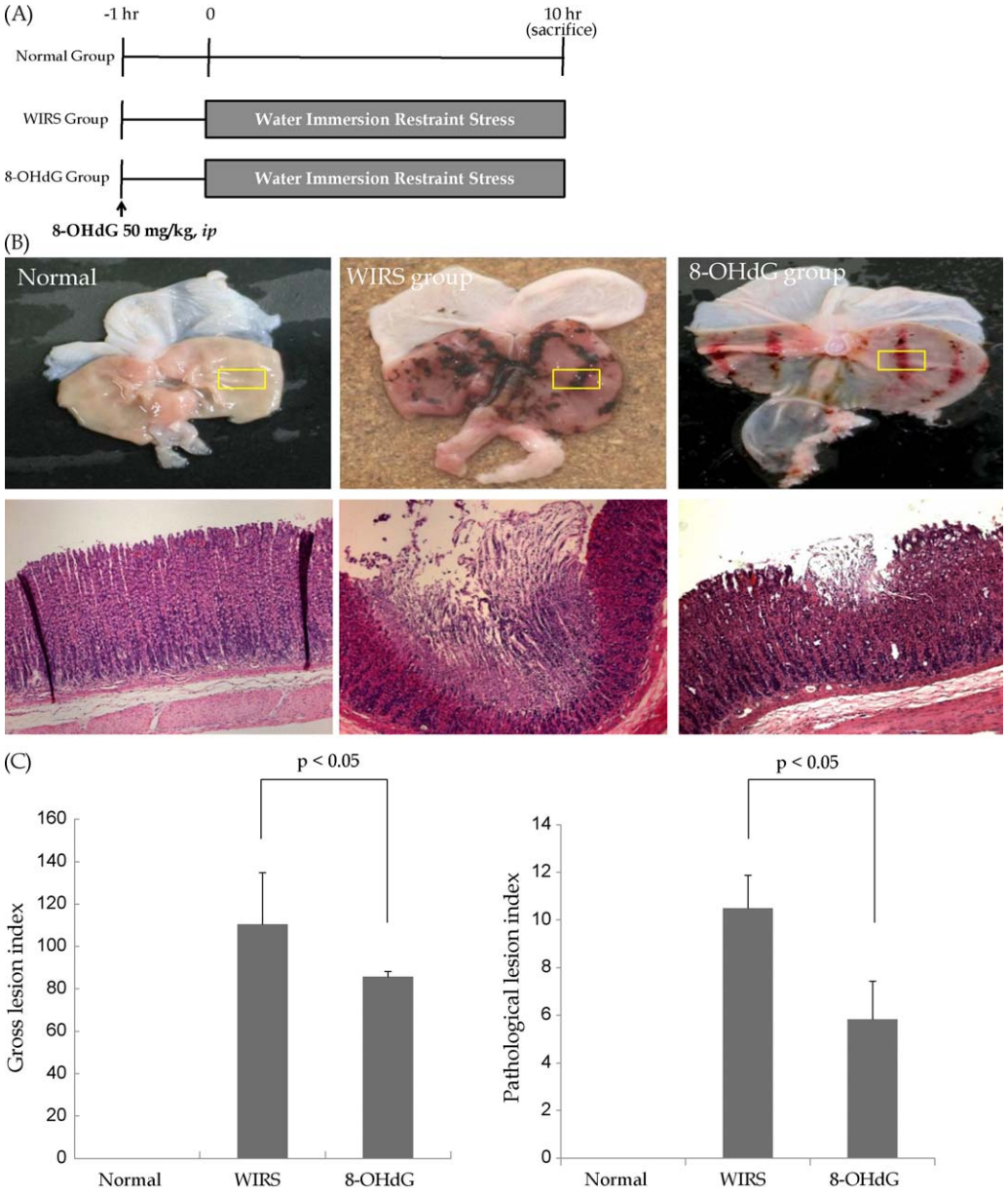

Fig. 6. 8-OHdG efficacy in the WIRS rat model. (A) A schematic view of the experimental protocol. WIRS was administered for 10 h to produce hemorrhagic gastritis. No mortality occurred during the WIRS experiment. (B) Gross and microscopic pathologies in the Normal, WIRS control, WIRS plus 8-OHdG (50 mg/kg) groups. WIRS for 10 h induced hemorrhagic gastritis and ulcers, whereas only erosive changes were noted in the WIRS plus 8-OHdG group. (C) Gross lesion index and pathologic lesion index of three groups were measured. Gross lesion index was defined as the number of ulcer formation, and the definition of pathologic lesion index was described in "Section 2". (D) The mucosal protein levels of TNF-α, IL-1β, VEGF, PGE_2, and gastrin I and the serum level of total nitrate was assayed by ELISA methods. Mucosal levels of TNF-α and VEGF were significantly lower in the WIRS plus 8-OHdG group than in the WIRS group ($p < 0.05$).

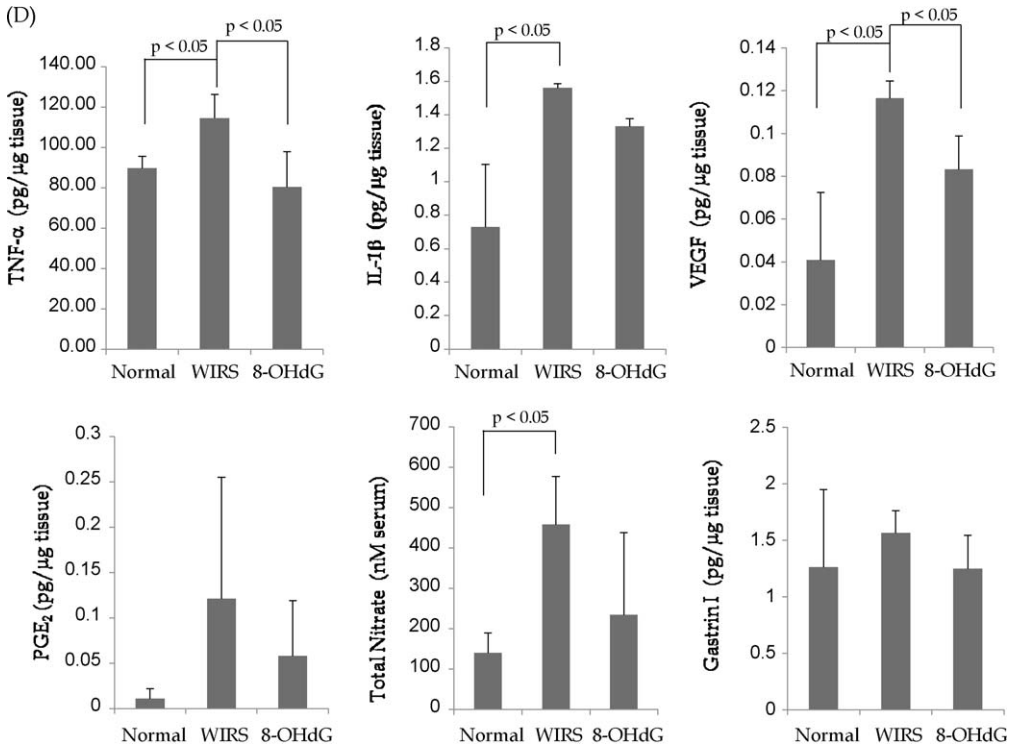

Fig. 6. (*Continued*).

creased over past decades, it is still one of the main concerns in an intensive care unit setting [22]. Endoscopic studies show that 75–100% of critically ill patients develop a gross gastric lesion within the first 1–3 days of illness, and almost all patients who are extremely ill have a SRMD [57,58]. Furthermore, severe SRMD, which often causes upper gastrointestinal (GI) bleeding, is associated with significant mortality [59]. Although the pathophysiologic mechanism of SRMD has not been clarified, it appears to be related to local ischemia followed by reperfusion injury. The main detrimental effect of reperfusion injury is known to be mediated by oxidative stress induced by abundantly oxygenated blood flow [60]. In the present study, we found that 8-OHdG had marked effects on a WIRS rat model, and that this effect was comparable to that achieved by conventional drugs, such as, rebamipide and *A. asiatica* extracts. Though not shown in this analysis, a dose-dependent improvement in WIRS-induced gastric lesions was noted in animals treated with a higher dose of 8-OHdG 100 mg/kg. Several types of therapeutics have been examined as treatments for stress-associated gastritis or gastric ulcers. These include *H. pylori* eradication, cetrexate, vitamin E, PPI, misoprostol, sucralfate, H_2 receptor antagonist, and rebamipide. However, these agents only limited the damage caused, and no agent has yet been found that addresses the underlying pathophysiologic abnormalities of SRMDs.

Based on results obtained in the present study, we hope to design a strategy based on exogenous 8-OHdG that corrects underlying pathophysiologic derangements associated with SRMDs. In addition, we believe that 8-OHdG has the potential to treat or prevent diseases caused by bouts of oxidative stress or inflammation. However, further verification and well-designed trials are required.

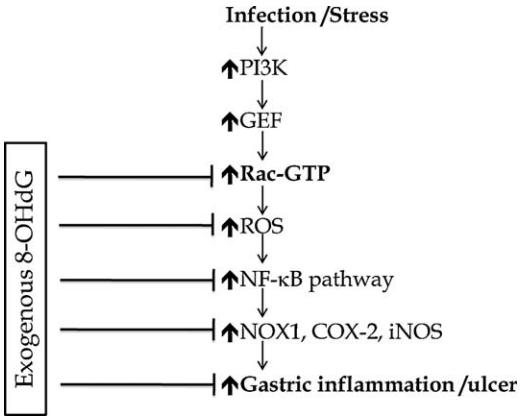

Fig. 7. Schematic review showing the signal pathway related to the LPS/stress induced redox-sensitive inflammatory cascade and the effect of 8-OHdG intervention. LPS activates PI3K, which activates Rac-GEF. Activated Rac-GEF catalyzes GDP-GTP translocation, which increases Rac-GTP binding, which activates NOX, and NOX generates ROS. Abundant ROS activates the NF-κB pathway, which increases the expressions of the redox-related inflammatory mediators, NOX1, COX2, iNOS, and others. 8-OHdG interferes with Rac-GTP binding, possibly by competitive inhibition, thereby preventing inflammation cascades and oxidative stress-associated gastric mucosal damage.

Acknowledgement

We thank J.H. Kim, PhD (SK Chemical R&D Institute, Suwon, Korea) for helping the animal experiment for the current study and the current study was granted from the Cancer Control R&D, the Ministry of Health and Welfare.

Appendix A. Supplementary data

Supplementary data associated with this article can be found, in the online version, at doi:10.1016/j.bcp.2010.08.023.

References

[1] Asami S, Manabe H, Miyake J, Tsurudome Y, Hirano T, Yamaguchi R, et al. Cigarette smoking induces an increase in oxidative DNA damage, 8-hydroxydeoxyguanosine, in a central site of the human lung. Carcinogenesis 1997;18:1763–6.

[2] Nakabeppu Y, Sakumi K, Sakamoto K, Tsuchimoto D, Tsuzuki T, Nakatsu Y. Mutagenesis and carcinogenesis caused by the oxidation of nucleic acids. Biol Chem 2006;387:373–9.
[3] Shibutani S, Takeshita M, Grollman AP. Insertion of specific bases during DNA synthesis past the oxidation-damaged base 8-oxodG. Nature 1991;349:431–4.
[4] Moriya M. Single-stranded shuttle phagemid for mutagenesis studies in mammalian cells: 8-oxoguanine in DNA induces targeted G.C → T.A transversions in simian kidney cells. Proc Natl Acad Sci USA 1993;90:1122–6.
[5] Weimann A, Riis B, Poulsen HE. Oligonucleotides in human urine do not contain 8-oxo-7,8-dihydrodeoxyguanosine. Free Radic Biol Med 2004;36: 1378–1382.
[6] Reardon JT, Bessho T, Kung HC, Bolton PH, Sancar A. In vitro repair of oxidative DNA damage by human nucleotide excision repair system: possible explanation for neurodegeneration in xeroderma pigmentosum patients. Proc Natl Acad Sci USA 1997;94:9463–8.
[7] Cooke MS, Evans MD, Dove R, Rozalski R, Gackowski D, Siomek A, et al. DNA repair is responsible for the presence of oxidatively damaged DNA lesions in urine. Mutat Res 2005;574:58–66.
[8] Martinet W, Knaapen MW, De Meyer GR, Herman AG, Kockx MM. Elevated levels of oxidative DNA damage and DNA repair enzymes in human atherosclerotic plaques. Circulation 2002;106:927–32.
[9] Kanauchi M, Nishioka H, Hashimoto T. Oxidative DNA damage and tubulointerstitial injury in diabetic nephropathy. Nephron 2002;91:327–9.
[10] Musarrat J, Arezina-Wilson J, Wani AA. Prognostic and aetiological relevance of 8-hydroxyguanosine in human breast carcinogenesis. Eur J Cancer 1996;32A: 1209–14.
[11] Wu LL, Chiou CC, Chang PY, Wu JT. Urinary 8-OHdG: a marker of oxidative stress to DNA and a risk factor for cancer, atherosclerosis and diabetics. Clin Chim Acta 2004;339:1–9.
[12] Hahm KB, Lee KJ, Choi SY, Kim JH, Cho SW, Yim H, et al. Possibility of chemoprevention by the eradication of Helicobacter pylori: oxidative DNA damage and apoptosis in H. pylori infection. Am J Gastroenterol 1997;92: 1853–1857.
[13] Yoon SH, Hyun JW, Choi J, Choi EY, Kim HJ, Lee SJ, et al. In vitro evidence for the recognition of 8-oxoGTP by Ras, a small GTP-binding protein. Biochem Biophys Res Commun 2005;327:342–8.
[14] Kim DH, Cho IH, Kim HS, Jung JE, Kim JE, Lee KH, et al. Anti-inflammatory effects of 8-hydroxydeoxyguanosine in LPS-induced microglia activation: suppression of STAT3-mediated intercellular adhesion molecule-1 expression. Exp Mol Med 2006;38:417–27.
[15] Choi S, Choi HH, Lee SH, Ko SH, You HJ, Ye SK, et al. Anti-inflammatory effects of 8-hydroxy-2′-deoxyguanosine on lipopolysaccharide-induced inflammation via Rac suppression in Balb/c mice. Free Radic Biol Med 2007;43:1594–603.
[16] Cheng G, Diebold BA, Hughes Y, Lambeth JD. Nox1-dependent reactive oxygen generation is regulated by Rac1. J Biol Chem 2006;281:17718–26.
[17] Park EJ, Ji KA, Jeon SB, Choi WH, Han IO, You HJ, et al. Rac1 contributes to maximal activation of STAT1 and STAT3 in IFN-gamma-stimulated rat astrocytes. J Immunol 2004;173:5697–703.
[18] Sulciner DJ, Irani K, Yu ZX, Ferrans VJ, Goldschmidt-Clermont P, Finkel T. rac1 regulates a cytokine-stimulated, redox-dependent pathway necessary for NF-kappaB activation. Mol Cell Biol 1996;16:7115–21.
[19] Burridge K, Wennerberg K. Rho and Rac take center stage. Cell 2004;116: 167–79.
[20] Murga C, Zohar M, Teramoto H, Gutkind JS. Rac1 and RhoG promote cell survival by the activation of PI3K and Akt, independently of their ability to stimulate JNK and NF-kappaB. Oncogene 2002;21:207–16.
[21] Embade N, Valeron PF, Aznar S, Lopez-Collazo E, Lacal JC. Apoptosis induced by Rac GTPase correlates with induction of FasL and ceramides production. Mol Biol Cell 2000;11:4347–58.
[22] Choung RS, Talley NJ. Epidemiology and clinical presentation of stress-related peptic damage and chronic peptic ulcer. Curr Mol Med 2008;8:253–7.
[23] Kamada T, Sato N, Kawano S, Fusamoto H, Abe H. Gastric mucosal hemodynamics after thermal or head injury. A clinical application of reflectance spectrophotometry. Gastroenterology 1982;83:535–40.
[24] Leung FW, Itoh M, Hirabayashi K, Guth PH. Role of blood flow in gastric and duodenal mucosal injury in the rat. Gastroenterology 1985;88:281–9.
[25] Maricic N, Ehrlich K, Gretzer B, Schuligoi R, Respondek M, Peskar BM. Selective cyclo-oxygenase-2 inhibitors aggravate ischaemia-reperfusion injury in the rat stomach. Br J Pharmacol 1999;128:1659–66.
[26] Koong AC, Chen EY, Giaccia AJ. Hypoxia causes the activation of nuclear factor kappa B through the phosphorylation of I kappa B alpha on tyrosine residues. Cancer Res 1994;54:1425–30.
[27] Maulik N, Das DK. Redox signaling in vascular angiogenesis. Free Radic Biol Med 2002;33:1047–60.
[28] Yamamoto N, Sakagami T, Fukuda Y, Koizuka H, Hori K, Sawada Y, et al. Influence of Helicobacter pylori infection on development of stress-induced gastric mucosal injury. J Gastroenterol 2000;35:332–40.
[29] Oh TY, Yeo M, Han SU, Cho YK, Kim YB, Chung MH, et al. Synergism of Helicobacter pylori infection and stress on the augmentation of gastric mucosal damage and its prevention with alpha-tocopherol. Free Radic Biol Med 2005;38:1447–57.
[30] Kuchino Y, Mori F, Kasai H, Inoue H, Iwai S, Miura K, et al. Misreading of DNA templates containing 8-hydroxydeoxyguanosine at the modified base and at adjacent residues. Nature 1987;327:77–9.
[31] Rossman KL, Der CJ, Sondek J. GEF means go: turning on RHO GTPases with guanine nucleotide-exchange factors. Nat Rev Mol Cell Biol 2005;6:167–80.
[32] Karnoub AE, Worthylake DK, Rossman KL, Pruitt WM, Campbell SL, Sondek J, et al. Molecular basis for Rac1 recognition by guanine nucleotide exchange factors. Nat Struct Biol 2001;8:1037–41.
[33] Welch HC, Coadwell WJ, Stephens LR, Hawkins PT. Phosphoinositide 3-kinase-dependent activation of Rac. FEBS Lett 2003;546:93–7.
[34] Yabana T, Yachi A. Stress-induced vascular damage and ulcer. Dig Dis Sci 1988;33:751–61.
[35] Hamaguchi M, Watanabe T, Higuchi K, Tominaga K, Fujiwara Y, Arakawa T. Mechanisms and roles of neutrophil infiltration in stress-induced gastric injury in rats. Dig Dis Sci 2001;46:2708–15.
[36] Balaban RS, Nemoto S, Finkel T. Mitochondria, oxidants, and aging. Cell 2005;120:483–95.
[37] Gonzalez FJ. Role of cytochromes P450 in chemical toxicity and oxidative stress: studies with CYP2E1. Mutat Res 2005;569:101–10.
[38] Schrader M, Fahimi HD. Mammalian peroxisomes and reactive oxygen species. Histochem Cell Biol 2004;122:383–93.
[39] Bedard K, Krause KH. The NOX family of ROS-generating NADPH oxidases: physiology and pathophysiology. Physiol Rev 2007;87:245–313.
[40] Han J, Luby-Phelps K, Das B, Shu X, Xia Y, Mosteller RD, et al. Role of substrates and products of PI 3-kinase in regulating activation of Rac-related guanosine triphosphatases by Vav. Science 1998;279:558–60.
[41] Welch HC, Coadwell WJ, Ellson CD, Ferguson GJ, Andrews SR, Erdjument-Bromage H, et al. P-Rex1, a PtdIns(3,4,5)P3- and Gbetagamma-regulated guanine-nucleotide exchange factor for Rac. Cell 2002;108:809–21.
[42] Royer-Pokora B, Kunkel LM, Monaco AP, Goff SC, Newburger PE, Baehner RL, et al. Cloning the gene for an inherited human disorder – chronic granulomatous disease – on the basis of its chromosomal location. Nature 1986;322: 32–8.
[43] Teahan C, Rowe P, Parker P, Totty N, Segal AW. The X-linked chronic granulomatous disease gene codes for the beta-chain of cytochrome b-245. Nature 1987;327:720–1.
[44] Szanto I, Rubbia-Brandt L, Kiss P, Steger K, Banfi B, Kovari E, et al. Expression of NOX1, a superoxide-generating NADPH oxidase, in colon cancer and inflammatory bowel disease. J Pathol 2005;207:164–76.
[45] Lassegue B, Sorescu D, Szocs K, Yin Q, Akers M, Zhang Y, et al. Novel gp91(phox) homologues in vascular smooth muscle cells: nox1 mediates angiotensin II-induced superoxide formation and redox-sensitive signaling pathways. Circ Res 2001;88:888–94.
[46] Ago T, Kitazono T, Kuroda J, Kumai Y, Kamouchi M, Ooboshi H, et al. NAD(P)H oxidases in rat basilar arterial endothelial cells. Stroke 2005;36:1040–6.
[47] Frey RS, Ushio-Fukai M, Malik AB. NADPH oxidase-dependent signaling in endothelial cells: role in physiology and pathophysiology. Antioxid Redox Signal 2009;11:791–810.
[48] Sedeek M, Hebert RL, Kennedy CR, Burns KD, Touyz RM. Molecular mechanisms of hypertension: role of Nox family NADPH oxidases. Curr Opin Nephrol Hypertens 2009;18:122–7.
[49] Rokutan K, Kawahara T, Kuwano Y, Tominaga K, Nishida K, Teshima-Kondo S. Nox enzymes and oxidative stress in the immunopathology of the gastrointestinal tract. Semin Immunopathol 2008;30:315–27.
[50] Kawahara T, Kohjima M, Kuwano Y, Mino H, Teshima-Kondo S, Takeya R, et al. Helicobacter pylori lipopolysaccharide activates Rac1 and transcription of NADPH oxidase Nox1 and its organizer NOXO1 in guinea pig gastric mucosal cells. Am J Physiol Cell Physiol 2005;288:C450–7.
[51] Berendes H, Bridges RA, Good RA. A fatal granulomatosus of childhood: the clinical study of a new syndrome. Minn Med 1957;40:309–12.
[52] Quie PG, White JG, Holmes B, Good RA. In vitro bactericidal capacity of human polymorphonuclear leukocytes: diminished activity in chronic granulomatous disease of childhood. J Clin Invest 1967;46:668–79.
[53] Banfi B, Clark RA, Steger K, Krause KH. Two novel proteins activate superoxide generation by the NADPH oxidase NOX1. J Biol Chem 2003;278:3510–3.
[54] Heuser I, Lammers CH. Stress and the brain. Neurobiol Aging 2003;24(Suppl. 1):S69–76. discussion S81–2.
[55] Selye H. A syndrome produced by diverse nocuous agents. 1936. J Neuropsychiatry Clin Neurosci 1998;10:230–1.
[56] Anderberg B, Sjodahl R. Prophylaxis and management of stress ulcers. Scand J Gastroenterol Suppl 1985;110:101–4.
[57] Peura DA, Johnson LF. Cimetidine for prevention and treatment of gastroduodenal mucosal lesions in patients in an intensive care unit. Ann Intern Med 1985;103:173–7.
[58] Lucas CE, Sugawa C, Riddle J, Rector F, Rosenberg B, Walt AJ. Natural history and surgical dilemma of "stress" gastric bleeding. Arch Surg 1971;102:266–73.
[59] Cook DJ, Fuller HD, Guyatt GH, Marshall JC, Leasa D, Hall R, et al. Risk factors for gastrointestinal bleeding in critically ill patients. Canadian Critical Care Trials Group. N Engl J Med 1994;330:377–81.
[60] Misra MK, Sarwat M, Bhakuni P, Tuteja R, Tuteja N. Oxidative stress and ischemic myocardial syndromes. Med Sci Monit 2009;15:RA209–1.